Article

Cobalt Minimisation in Violet $Co_3P_2O_8$ Pigment

Mª Ángeles Tena [1,*], Rafael Mendoza [2], Camino Trobajo [3] and Santiago García-Granda [4,*]

[1] Inorganic Chemistry Area, Inorganic and Organic Chemistry Department, Jaume I University, P.O. Box 224, 12006 Castellón, Spain

[2] Physical Chemistry Area, Scientific and Technical Services, Oviedo University-CINN, 33006 Oviedo, Spain; mendozarafael@uniovi.es

[3] Inorganic Chemistry Area, Organic and Inorganic Chemistry Department, Oviedo University-CINN, 33006 Oviedo, Spain; ctf@uniovi.es

[4] Physical Chemistry Area, Physical and Analytical Chemistry Department, Oviedo University-CINN, 33006 Oviedo, Spain

[*] Correspondence: tena@uji.es (M.Á.T.); s.garciagranda@cinn.es (S.G.-G.)

Abstract: This study considers the limitations of cobalt violet orthophosphate, $Co_3P_2O_8$, in the ceramic industry due to its large amount of cobalt. $Mg_xCo_{3-x}P_2O_8$ ($0 \leq x \leq 3$) solid solutions with the stable $Co_3P_2O_8$ structure were synthesised via the chemical coprecipitation method. The formation of solid solutions between the isostructural $Co_3P_2O_8$ and $Mg_3P_2O_8$ compounds decreased the toxically large amount of cobalt in this inorganic pigment and increased the melting point to a temperature higher than 1200 °C when $x \geq 1.5$. $Co_3P_2O_8$ melted at 1160 °C, and compositions with $x \geq 1.5$ were stable between 800 and 1200 °C. The substitution of Co(II) with Mg(II) decreased the toxicity of these materials and decreased their price; hence, the interest of these materials for the ceramic industry is greater. An interesting purple colour with a* = 31.6 and b* = −24.2 was obtained from a powdered $Mg_{2.5}Co_{0.5}P_2O_8$ composition fired at 1200 °C. It considerably reduced the amount of cobalt, thus improving the colour of the $Co_3P_2O_8$ pigment (a* = 16.2 and b* = −20.1 at 1000 °C). $Co_3P_2O_8$ is classified as an inorganic pigment (DCMA-8-11-1), and the solid solutions prepared were also inorganic pigments when unglazed. When introducing 3% of the sample (pigment) together with enamel, spreading the mixture on a ceramic support and calcining the whole in an electric oven, a colour change from violet to blue was observed due to the change in the local environment of Co(II), which could be seen in the UVV spectra of the glazed samples with the displacement of the bands towards higher wavelengths and with the appearance of a new band assigned to tetrahedral Co(II). This blue colour was also obtained with Co_2SiO_4, $MgCoSiO_4$ or $Co_3P_2O_8$ pigments containing a greater amount of cobalt.

Keywords: minimisation of toxicity; $Co_3P_2O_8$; α-$Mg_3P_2O_8$; solid solutions; pigments

1. Introduction

In the ceramic industry, dark blue is obtained by using compounds or solid solutions containing cobalt. The coordination number of the Co(II) cation is different among the crystalline structures used, and the colouration of powdered compositions changes between blue ($CoAl_2O_4$ with a spinel structure and 88% tetrahedral Co(II), ICSD-260589; $Co_xZn_{2-x}SiO_4$ ($0.005 \leq x \leq 1$) with a willemite structure, and 100% tetrahedral Co(II) ICSD-186367) and violet, blue, or purple (Co_2SiO_4 with olivine structure and 100% octahedral Co(II) ICSD-260092; $Co_3P_2O_8$ with a related olivine structure and 100% octahedral Co(II) ICSD-9850; stable $Co_3P_2O_8$ with 1/3 octahedral Co(II) and 2/3 Co(II) in C.N. = 5 ICSD-38259) [1].

Cobalt violet orthophosphate, $Co_3P_2O_8$, is a pigment included in the DCMA Classification of Mixed Metal Oxide Inorganic Colour Pigments (DCMA-8-11-1) [2]. Its use in the ceramic industry is limited because of the large amount of cobalt in this compound. The

formation of solid solutions between the isostructural $Co_3P_2O_8$ and $Mg_3P_2O_8$ compounds could be used to avoid the toxically large amount of cobalt in this pigment. In compositions that are rich in magnesium, these solid solutions could decrease the amount of cobalt, thus increasing the interest of these materials for the ceramic industry. The substitution of Co(II) with Mg(II) decreases the toxicity of these materials and decreases their price. The $Co_3P_2O_8$ compound melts at 1160 °C [3,4]. Magnesium orthophosphate melts at 1357 °C [5]. The melting point of some compositions of the solid solutions could be higher than 1200 °C.

The formation of solid solutions through the substitution of ions in a crystalline structure changes the bond strength and modifies the colour of the materials. The colour blue is usually obtained from a tetrahedral CoO_4 geometry. The colour purple is obtained from $LiZn_{1-x}Co_xPO_4$ ($0 \leq x \leq 0.4$) compositions with a $LiZnPO_4$ structure, which can be explained by the highly distorted geometry in the CoO_4 tetrahedra. The shorter Co-O bonds increase the ligand field strength and lead to a blue-shifted absorption, thus developing an excellent purple pigment [6]. The increase in the amount of Co in these compositions decreases the negative b* value of the CIE L* a* b* parameters and the colour change to a violet hue due to the presence of the $LiCoPO_4$ phase with Co(II) ions in octahedral coordination together with the $LiZnPO_4$ phase with Co(II) ions in tetrahedral coordination [6].

The stable polymorph of the $Co_3P_2O_8$ compound with the monoclinic $Mg_3P_2O_8$ structure (α phase) contains Co(II) ions in both a square planar pyramid and an octahedral coordination, Co1 in the 4e site and Co2 in the 2a site (ICSD-38259) [7]. A polymorph of the $Mg_3P_2O_8$ compound with the $Ni_3P_2O_8$ structure (β phase) has also been reported (ICSD-9849) [1,8]. The transition temperature from β-$Mg_3P_2O_8$ to α-$Mg_3P_2O_8$ (ICSD-261231) is 1055 °C [5]. In the stable $Co_3P_2O_8$ structure, all of the Co(II) ions are distributed in layers (bc planes), and these layers are joined by PO_4 tetrahedra. Figure 1 shows two unit cells of the stable $Co_3P_2O_8$ structure, the projection of nine unit cells in the (001) plane and the details of the oxygens around Co1 (CN = 5) and Co2 (CN = 6), with an edge shared by both polyhedra (two oxygens, O1 and O2, shared between Co1 and Co2). Two Co1-to-Co2 distances—2.896 and 3.165 Å—are shorter than the other Co-to-Co distances (ICSD-38259) [7]. The structure was drawn with the FPStudio program [9–11].
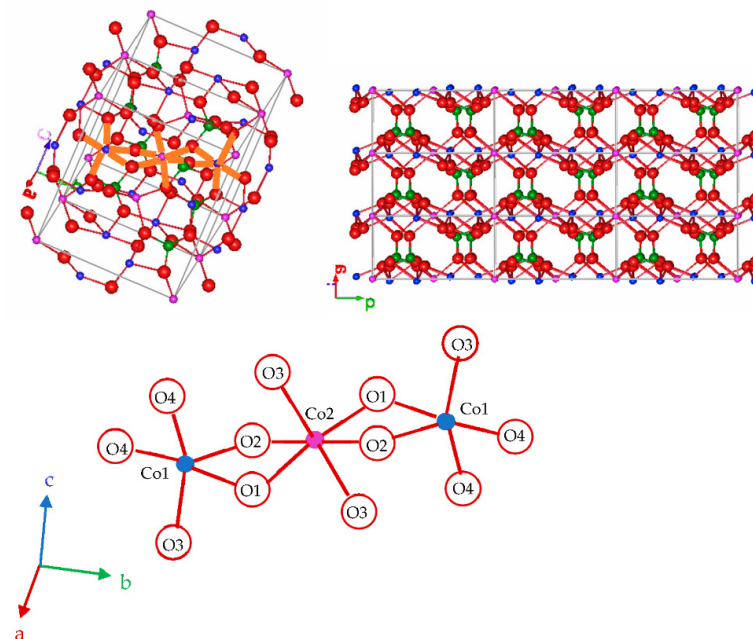
Figure 1. Stable $Co_3P_2O_8$ structure. The colour scheme to represent the atoms is O (-II): red, P(V): green, Co(II): blue with CN = 5, and lilac with CN = 6.

Cobalt orthophosphate is soluble in $Mg_3(PO_4)_2$ at about 1100 K (827 °C) over the whole range of compositions [12]. Information about $(Co, Mg)_3(PO_4)_2$ solid solutions with the α-$Mg_3P_2O_8$ structure prepared from mixtures of $Co_3P_2O_8$ and $Mg_3P_2O_8$ orthophosphates and fired at 800 °C can be found in the bibliography [13]. The catalytic behaviour of $Mg_{3-x}Co_x(PO_4)_2$ solid solutions (compositions fired at 500–700 °C) shows that the substitution of magnesium with cobalt in the $Mg_3(PO_4)_2$ structure leads to active and selective phases in the oxidative dehydrogenation of ethane and propane [14]. It seems possible to increase the thermal stability of $Co_3P_2O_8$ through the formation of these solid solutions with the substitution of Co(II) ions by Mg(II) ions. As far as we know, no information about $Mg_xCo_{3-x}P_2O_8$ solid solutions at T $\geq$ 1000 °C has been reported.

In $Co_{2-x}Zn_xSiO_4$ solid solutions comprising Co_2SiO_4 and Zn_2SiO_4 compounds with olivine and willemite structures, the intense blue colour is kept with a considerably lower amount of cobalt [15]. In the same way, the colour of some compositions of solid solutions with the structure of cobalt orthophosphate with a small amount of cobalt could also be similar to the colour of the $Co_3P_2O_8$ compound. It was expected that the change in the coordination number of the Co(II) ion would modify the colouration of the material with respect to that obtained with the olivine and willemite structures.

The aim of this study was the formation of solid solutions from compositions comprising $Co_3P_2O_8$ and $Mg_3P_2O_8$ in order to obtain information about the composition and temperature with which the desired colour is developed and to minimise the toxic and expensive amounts of cobalt.

2. Experimental Methods

$Mg_xCo_{3-x}P_2O_8$ ($0 \leq x \leq 3$) compositions were synthesised from $MgCl_2 \cdot 6H_2O$ (Scharlau, extra pure), $Co(NO_3)_2 \cdot 6H_2O$ (Acros Organic, 99%) and H_3PO_4 (Merck, 99%) via the chemical coprecipitation method.

Stoichiometric amounts of $MgCl_2 \cdot 6H_2O$, $Co(NO_3)_2 \cdot 6H_2O$ and a 0.5 M solution of H_3PO_4 in water were added to 100 mL of water. Samples were vigorously stirred for 20 h at room temperature. Then, an aqueous ammonia solution (Panreac, 25%) was added under continuous stirring until reaching pH = 10. The experimental parameters were chosen in order to obtain precipitates of the cations before drying the material. pH = 10 was chosen because, although $Co(OH)_2$ precipitates at pH > 7, $Mg(OH)_2$ precipitates at pH > 9.5. Under these conditions, the materials were coprecipitated and dried in a stove at 65 °C to evacuate only the water. The Mg:Co:P molar ratio of the starting materials was preserved in this process. The dry samples were fired at 300, 600, 800, 1000 and 1200 °C for 6 h at each temperature.

The development of the crystalline phases at different temperatures was studied by using XRD. The resulting materials were examined using a Panalytical X-ray diffractometer (Malvern Panalytical, Almelo, The Netherlands) with CuK_α radiation. A structure profile refinement was carried out using the Rietveld method (Fullprof.2k computer program) [9–11]. Diffraction patterns ranging between 6 and 110 (2θ) were collected by employing monochromatic CuK_α radiation, a step size of 0.02 (2θ) and a sampling time of 10 s. The unit cell parameters, interatomic distances and Co(II) ion occupation in the two M1 and M2 sites in the stable $Co_3P_2O_8$ structure were determined in order to investigate the possible formation of solid solutions under these synthesis conditions. The initial structural information was taken from the Inorganic Crystal Structure Database [1].

The Co(II) ion sites and the transfer charge bands in the samples were studied by using UV–vis–NIR spectroscopy (diffuse reflectance). The ultraviolet–visible–near-infrared (UV–vis–NIR) spectra in the range of 200 to 2500 nm were obtained using a Jasco V-670 spectrophotometer and $BaSO_4$ as reference substance.

The CIEL*a*b* colour parameters for the fired samples—L* is the lightness axis (black (0) $\rightarrow$ white (100)), a* is the green ($-$) $\rightarrow$ red (+) axis and b* is the blue ($-$) $\rightarrow$ yellow (+) axis [16]—were obtained with an X-Rite spectrophotometer (SP60, standard illuminant: D65, an observer of 10°, and a reference sample of MgO).

To test their possible utility in the ceramic industry, the compositions fired at 1200 °C were enamelled at 3% weight with a commercial glaze (SiO_2–Al_2O_3–PbO–Na_2O–CaO glaze) onto commercial ceramic biscuits. Many pigments were dissolved in this glaze. The colour of the material was lost when this occurred. Glazed tiles were fired for 15 min at 1065 °C, and subsequently, their UV–vis–NIR spectra and their CIEL*a*b* colour parameters were obtained.

3. Results and Discussion

Table 1 shows the evolution of the crystalline phases in the $Mg_xCo_{3-x}P_2O_8$ ($0.0 \leq x \leq 3.0$) compositions according to composition and temperature. A stable $Co_3P_2O_8$ structure was developed at 800 °C, although small amounts of $Mg_2P_2O_7$ were also detected when $x \geq 2.0$ at this temperature. This crystalline phase was the only crystalline phase detected in all of the compositions at 1000 °C and when $x \geq 1.5$ at 1200 °C. Compositions with $x < 1.5$ melted at 1200 °C, and they could not be removed from the crucible.

**Table 1.** Evolution of crystalline phases with temperature in the $Mg_xCo_{3-x}P_2O_8$ ($0.0 \leq x \leq 3.0$) compositions.

X	800 °C	1000 °C	1200 °C
0.0	C(s)	C(s)	
0.5	C(s)	C(s)	
1.0	C(s)	C(s)	
1.5	C(s)	C(s)	C(s)
2.0	C(s), M(vw)	C(s)	C(s)
2.5	C(s), M(vw)	C(s)	C(s)
3.0	C(s), M(w)	C(s)	C(s)

Crystalline phases: C = stable $Co_3P_2O_8$, $Mg_3P_2O_8$, or solid solutions with the same structure; M = $Mg_2P_2O_7$. Diffraction peak intensity: s = strong, vw = very weak.

The unit cell parameters, volumes and interatomic distances in the stable $Co_3P_2O_8$ structure (isostructural with the α-$Mg_3P_2O_8$ structure) were obtained from the $Mg_xCo_{3-x}P_2O_8$ ($0 \leq x \leq 3$) compositions by using Rietveld's method. Three examples of graphical results are shown in Figure 2. The changes in intensities due to compositional differences can be observed in this figure. Table 2 includes the unit cell parameters and volume, Table 3 includes the M-O (M = Mg, Co) distances, and Table 4 includes the P-O distances. The variations in the unit cell parameters in this structure at temperatures between 800 and 1200 °C are shown in Figures 3 and 4 shows the variations in the M-O and P-O distances at 1000 °C.

For the variations in the unit cell parameters with temperature, only small differences were detected when $x > 1.5$ (Figure 3). The decrease in the b unit cell parameter with x was consistent with the replacement of the Co(II) ion by the smaller Mg(II) ion (Table 2 and Figure 3). A slight negative departure of Vegard's law in the b parameter associated with short-range cation ordering [17] can be observed in Figure 3. The small increases obtained in the a and c unit cell parameters indicate a structural distortion produced when $Mg_xCo_{3-x}P_2O_8$ solid solutions were formed with the stable $Co_3P_2O_8$ structure. This structural distortion is in accordance with the opposite variation in the M1-O distances with the variation in the composition (x) that can be observed in Figure 4. The most remarkable variations were the decrease in M1-O1 (the longest distance) and the increase in M1-O3 with x when $x > 1.0$. At 1000 °C, the M-O distances were close to the Co-O distances in the $Co_3P_2O_8$ compound when $x \leq 1.5$, and the M-O distances were close to the Mg-O distances in the $Mg_3P_2O_8$ compound when $x > 1.5$. When the amount of Mg(II) ions increased, the difference between the shortest and longest distances was smaller than in compositions in which the amount of Co(II) ions was greater. A gradual variation in the M-O distances with x was obtained at 800 and 1000 °C, as well as in the compositions that did not melt at 1200 °C. The great distortion in the position with C.N. = 5 in $Co_3P_2O_8$ (with Co1-O distances between 1.940 and 2.286 Å according to the ICSD-38259 data) was kept in the

compositions in which $0.0 \leq x \leq 1.5$ at 800 and at 1000 °C. This distortion in the M1 site decreased in accordance with the values of the Mg1-O distances in $Mg_3P_2O_8$ (with Mg1-O distances between 1.969 and 2.150 Å according to the ICSD-261231 data). The differences in the electron configuration with the seven electrons in the 3d orbitals in the Co(II) ion and with a small orbital penetration effect could explain the fact that the Co-O distance (1.940 Å) was shorter than the Mg-O distance (1.969 Å), although the ionic radius was greater in the Co(II) ion than in the Mg(II) ion. The greater covalence in the Co-O bond than in the Mg-O bond could explain the shorter Co-O distances.
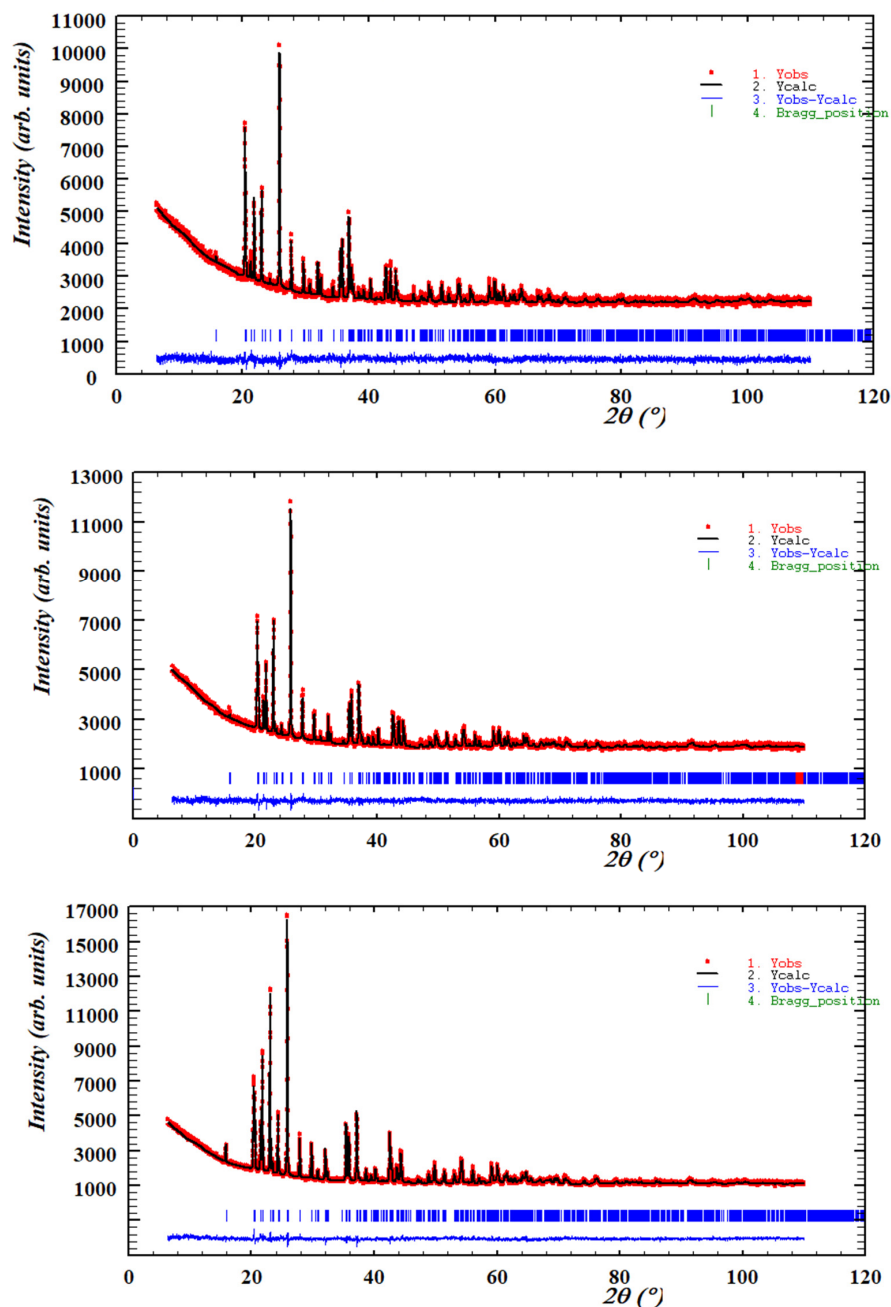
Figure 2. The diffraction profile refinement obtained with Rietveld's method for the $Mg_{0.5}Co_{2.5}P_2O_8$ (x = 0.5), $Mg_{1.5}Co_{1.5}P_2O_8$ (x = 1.5) and $Mg_{2.5}Co_{0.5}P_2O_8$ (x = 2.5) compositions fired at 1000 °C.

Table 2. Variations in unit cell parameters in the stable $Co_3P_2O_8$ structure obtained from fired $Mg_xCo_{3-x}P_2O_8$ ($0.0 \leq x \leq 3.0$) compositions.

| T (°C)	x	a (Å)	b (Å)	c (Å)	β (°)	V (Å³)
800	0.0	5.0629(1)	8.3618(2)	8.7888(2)	121.003(1)	318.92(1)
800	0.5	5.0655(1)	8.3377(2)	8.7938(2)	120.882(1)	318.75(1)
800	1.0	5.0691(1)	8.3131(1)	8.7999(2)	120.840(1)	318.40(1)
800	1.5	5.07242(9)	8.2887(1)	8.8076(1)	120.8274(9)	318.018(9)
800	2.0	5.07424(8)	8.2691(1)	8.8169(1)	120.8303(8)	317.675(8)
800	2.5	5.0734(1)	8.2505(2)	8.8237(2)	120.854(1)	317.07(1)
800	3.0	5.07529(9)	8.2370(1)	8.8316(2)	120.862(1)	316.93(1)
1000	0.0	5.06288(8)	8.3631(1)	8.7894(1)	120.9897(8)	319.027(8)
1000	0.5	5.06491(9)	8.3386(1)	8.7933(2)	120.8665(9)	318.78(1)
1000	1.0	5.0677(1)	8.3143(2)	8.7981(2)	120.820(1)	318.35(1)
1000	1.5	5.07022(8)	8.2914(1)	8.8056(1)	120.7983(8)	317.975(8)
1000	2.0	5.07251(6)	8.2704(1)	8.8146(1)	120.813(7)	317.588(7)
1000	2.5	5.07328(5)	8.25084(9)	8.82223(9)	120.8395(5)	317.073(6)
1000	3.0	5.07521(4)	8.23586(8)	8.83144(7)	120.8663(5)	316.860(5)
1200	1.5	5.07299(7)	8.2876(1)	8.8068(1)	120.8024(8)	318.034(7)
1200	2.0	5.07408(4)	8.26660(7)	8.81422(8)	120.8155(5)	317.520(5)
1200	2.5	5.07550(3)	8.24883(5)	8.82347(5)	120.8519(4)	317.139(3)
1200	3.0	5.07675(2)	8.23098(4)	8.83270(4)	120.8969(3)	316.712(3)

Table 3. Variations in the M-O (M = Co, Mg) distances in the stable $Co_3P_2O_8$ structure with temperature in the $Mg_xCo_{3-x}P_2O_8$ compositions.

T (°C)	X	M1-O1 (Å)	M1-O2 (Å)	M1-O3 (Å)	M1-O4 (Å)	M1-O4 (Å)	M2-O1 (x2) (Å)	M2-O2 (x2) (Å)	M2-O3 (x2) (Å)
800	0.0	2.274(6)	1.973(5)	2.065(7)	1.960(5)	1.996(5)	2.052(8)	2.195(4)	2.174(4)
800	0.5	2.273(6)	1.970(5)	2.076(7)	1.985(5)	1.992(5)	2.089(7)	2.184(4)	2.173(4)
800	1.0	2.253(5)	1.969(5)	2.070(7)	1.969(4)	1.999(4)	2.059(7)	2.183(4)	2.164(4)
800	1.5	2.246(5)	1.972(4)	2.074(6)	1.961(4)	1.995(4)	2.054(6)	2.185(3)	2.155(4)
800	2.0	2.242(5)	1.979(4)	2.091(6)	1.941(4)	1.985(4)	2.061(6)	2.188(3)	2.153(4)
800	2.5	2.228(5)	1.967(4)	2.102(4)	1.946(4)	1.991(4)	2.050(5)	2.187(3)	2.150(3)
800	3.0	2.226(5)	1.950(5)	2.098(6)	1.941(4)	1.980(4)	2.058(5)	2.182(3)	2.153(3)
1000	0.0	2.270(6)	1.977(5)	2.064(7)	1.969(5)	1.999(4)	2.057(7)	2.189(4)	2.172(4)
1000	0.5	2.265(6)	1.970(5)	2.069(7)	1.983(4)	1.992(4)	2.070(7)	2.188(4)	2.173(4)
1000	1.0	2.265(6)	1.961(5)	2.075(7)	1.967(5)	2.002(5)	2.058(7)	2.182(4)	2.171(4)
1000	1.5	2.246(5)	1.964(4)	2.072(6)	1.970(4)	1.997(4)	2.045(6)	2.179(3)	2.163(4)
1000	2.0	2.242(5)	1.972(4)	2.093(6)	1.954(4)	1.987(4)	2.057(6)	2.180(3)	2.158(4)
1000	2.5	2.190(4)	1.971(4)	2.088(5)	1.958(3)	1.986(4)	2.041(4)	2.177(3)	2.140(3)
1000	3.0	2.171(3)	1.960(3)	2.088(4)	1.953(3)	1.982(3)	2.035(3)	2.172(2)	2.138(2)
1200	1.5	2.229(6)	1.979(5)	2.078(7)	1.950(5)	1.983(5)	2.036(8)	2.201(4)	2.157(4)
1200	2.0	2.231(5)	1.956(4)	2.067(6)	1.965(4)	2.009(4)	2.037(6)	2.190(3)	2.171(4)
1200	2.5	2.203(4)	1.968(4)	2.085(5)	1.961(3)	2.000(4)	2.042(4)	2.162(3)	2.151(3)
1200	3.0	2.166(3)	1.956(3)	2.081(4)	1.965(3)	1.988(3)	2.033(3)	2.172(2)	2.138(2)

Table 4. Variations in the P-O distances in the stable $Co_3P_2O_8$ structure with temperature from the $Mg_xCo_{3-x}P_2O_8$ compositions.

T (°C)	X	P1-O1 (Å)	P1-O2 (Å)	P1-O3 (Å)	P1-O4 (Å)
800	0.0	1.944(9)	1.527(5)	1.561(5)	1.512(5)
800	0.5	1.521(9)	1.520(5)	1.566(5)	1.517(5)
800	1.0	1.512(9)	1.526(5)	1.550(5)	1.527(5)
800	1.5	1.516(8)	1.521(4)	1.546(4)	1.519(4)
800	2.0	1.518(7)	1.508(4)	1.537(4)	1.521(4)
800	2.5	1.516(7)	1.507(4)	1.534(3)	1.515(4)
800	3.0	1.524(6)	1.520(4)	1.544(3)	1.527(4)
1000	0.0	1.502(9)	1.524(5)	1.563(5)	1.517(5)
1000	0.5	1.513(9)	1.520(5)	1.560(5)	1.517(5)
1000	1.0	1.510(9)	1.518(5)	1.562(5)	1.520(5)
1000	1.5	1.513(7)	1.516(4)	1.548(4)	1.527(4)
1000	2.0	1.514(7)	1.508(4)	1.531(4)	1.515(4)
1000	2.5	1.519(5)	1.513(3)	1.543(3)	1.524(3)
1000	3.0	1.532(4)	1.522(3)	1.550(3)	1.532(3)
1200	1.5	1.516(9)	1.526(5)	1.522(5)	1.520(5)
1200	2.0	1.520(7)	1.483(4)	1.549(4)	1.526(4)
1200	2.5	1.505(5)	1.511(3)	1.537(3)	1.548(3)
1200	3.0	1.530(4)	1.516(3)	1.549(3)	1.527(3)
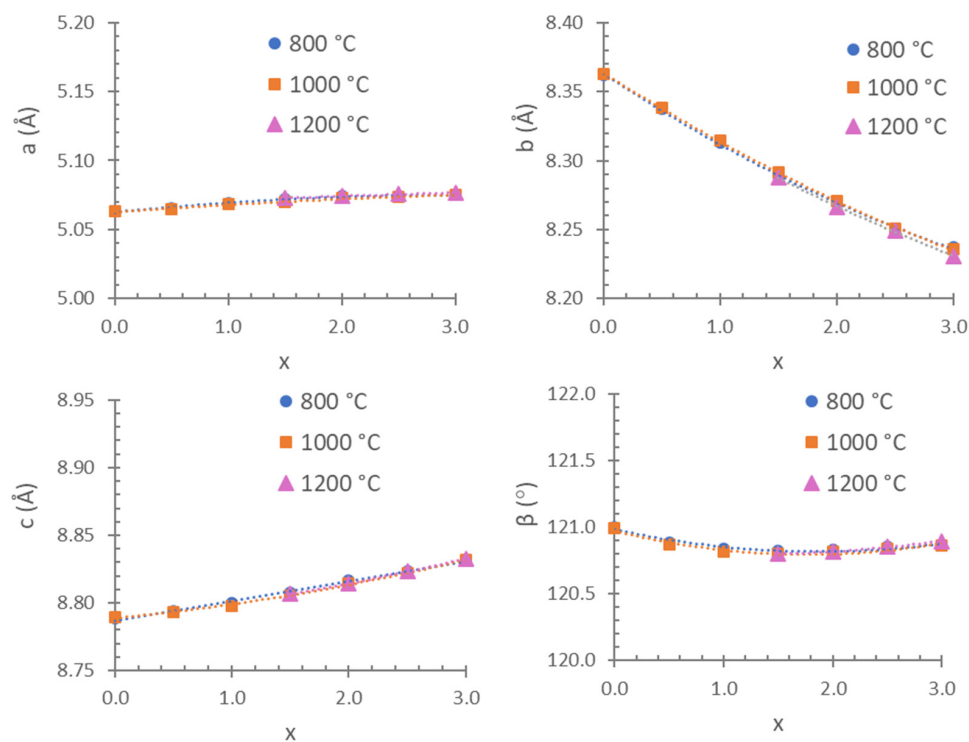
Figure 3. Unit cell parameters in the $Co_3P_2O_8$ structure from the $Mg_xCo_{3-x}P_2O_8$ ($0.0 \leq x \leq 3.0$) compositions fired at 800, 1000 and 1200 °C.
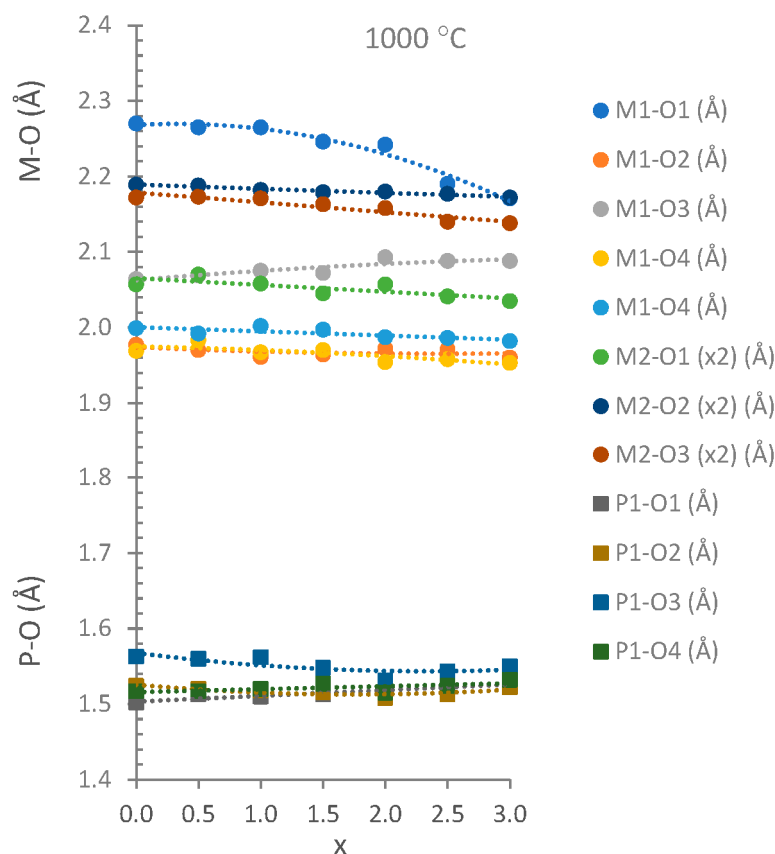
Figure 4. M-O (circles) and P-O (squares) distances in the stable $Co_3P_2O_8$ structure at 1000 °C.

Figure 5 shows the variations in the occupation of Co(II) ions in the 2a (M1) and 4e (M2) sites for the results of the DRX profile refined with the Rietveld method. The initial occupation of each position was calculated by dividing the multiplicity of this position by the multiplicity of the general position in the space group and multiplying that quotient by the value of $(3 - x)/3$. In accordance with the multiplicity of the sites, a random distribution of Co(II) ions between the M1 and M2 sites corresponded to a ratio of 4/4 = 1 (2/3 of the total Co(II) ions in the M1 site; general 4e position with C.N. = 5) and 2/4 = 0.5 (1/3 of the total Co(II) ions in the M2 site; special 2a position with C.N. = 6). The calculated values were refined, and the results appear in Figure 5 as E1 (experimental occupation in the M1 position) and E2 (experimental occupation in the M2 position). The experimental distribution of Co(II) between the two positions indicates that the Co(II) ion presents a higher preference for the site with C.N. = 5 (4e) than the Mg(II) ion at 800, 1000 and 1200 °C. The octahedral positions (2a) were mostly occupied by Mg(II) ions. This result is in agreement with the literature on compositions at 800 °C [12,13].

Figure 6 shows the UV–vis–NIR spectra of $Mg_xCo_{3-x}P_2O_8$ fired at 800, 1000 and 1200 °C. The three bands at 1100, 580 and 500 nm from the fired $Mg_xCo_{3-x}P_2O_8$ composition were assigned to Co(II) in the octahedral site with $\Delta/B < 13$. These bands could be assigned to the first $^4T_1 \rightarrow {}^4T_2(F)$ transition, to the second $^4T_1 \rightarrow {}^4A_2(F)$ transition and to the third $^4T_1 \rightarrow {}^4T_1(P)$ transition [18]. The bands at 1700–1717, 890 and 480 nm were assigned to Co(II) in a square-planar pyramid coordination ($^4A_2 \rightarrow {}^4A_1(F)$, $^4A_2 \rightarrow {}^4E(F)$ and $^4A_2 \rightarrow {}^4E(P)$ transitions) according to the stable $Co_3P_2O_8$ solid solutions detected by XRD.
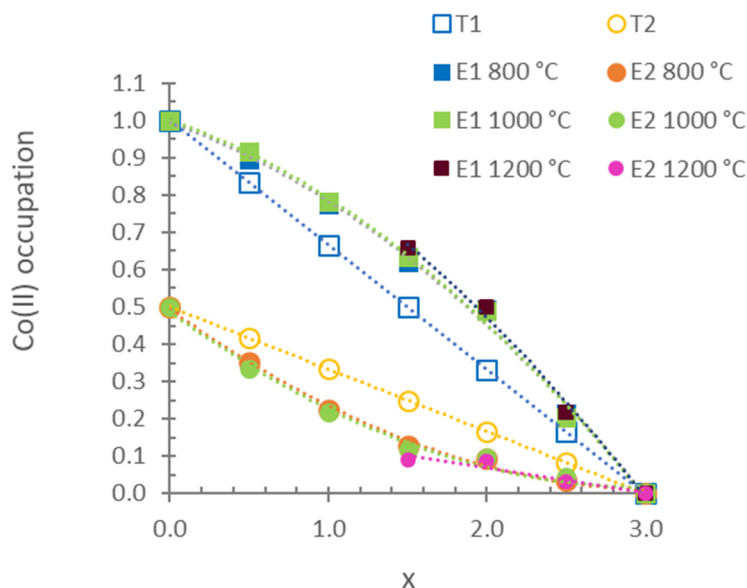
**Figure 5.** Variations in the occupation of Co(II) ions with composition in sites of the stable $Co_3P_2O_8$ structure from the fired $Mg_xCo_{3-x}P_2O_8$ compositions. E1: experimental occupation in pentacoordinated sites (M1), E2: experimental occupation in octahedral sites (M2), T1: theoretical random occupation in M1 sites and T2: theoretical random occupation in M2 sites.

In the spectra at 1000 °C, the absorbance at 1100 nm (the $^4T_1 \rightarrow {}^4T_2(F)$ transition was assigned to Co(II) in the octahedral site) was slightly smaller than at 890 nm (the $^4A_2 \rightarrow {}^4E(F)$ transition was assigned to Co(II) in a square-planar pyramid coordination) when x < 1.0 (small amount of Mg(II) in the compositions), although the most noticeable change was the decrease in absorbance with the composition due to the decrease in the total Co(II) in samples.

The slight changes in the Co-O distances with composition (Figure 4) changed the ligand field strength, and a gradation of purple to violet colour was obtained (Table 5). Purple and violet colours were obtained when the stable $Co_3P_2O_8$ structure was developed from these compositions. These colourations were kept at 1000 and 1200 °C when x ≥ 1.5, so pigments with a smaller amount of Co(II) were obtained.

According to the CIE L* a* b* parameters (Table 5), an increase in the amount of red colour could be detected starting at 600 °C with a* > 20 when 1.0 ≤ x ≤ 2.5 at 1000 °C. Figure 7 shows the variations in a* and b* with composition (x) at T ≥ 800 °C. All of the compositions with x ≠ 3.0 were violet or purple with a positive a* (red amount) and negative b* (blue amount). The composition with x = 1.5 ($Mg_{1.5}Co_{1.5}P_2O_8$) showed the greatest amounts of red and blue at 1000 °C, and the composition with x = 2.5 ($Mg_{2.5}Co_{0.5}P_2O_8$) did so at 1200 °C. The positions of the third transition band of the octahedral Co(II) ion, $^4T_1 \rightarrow {}^4T_1(P)$, and the $^4A_2 \rightarrow {}^4E(P)$ band of the Co(II) ion in a square-planar pyramid coordination could be related to the variation of the amount of red colour (positive a*). The amount of blue colour (negative b*) could be related to the second transition band of the octahedral Co(II) ion, $^4T_1 \rightarrow {}^4A_2$. The greatest amounts of red colour (positive a*) and blue colour (negative b*) were obtained when the totality of Co(II) was almost entirely in the pentacoordinated site (x > 1.0), with a great distortion at 1200 °C (Table 3). The optimal compositions could be established when 2.0 ≤ x ≤ 2.5 (highest a* and lowest b*) at this temperature.
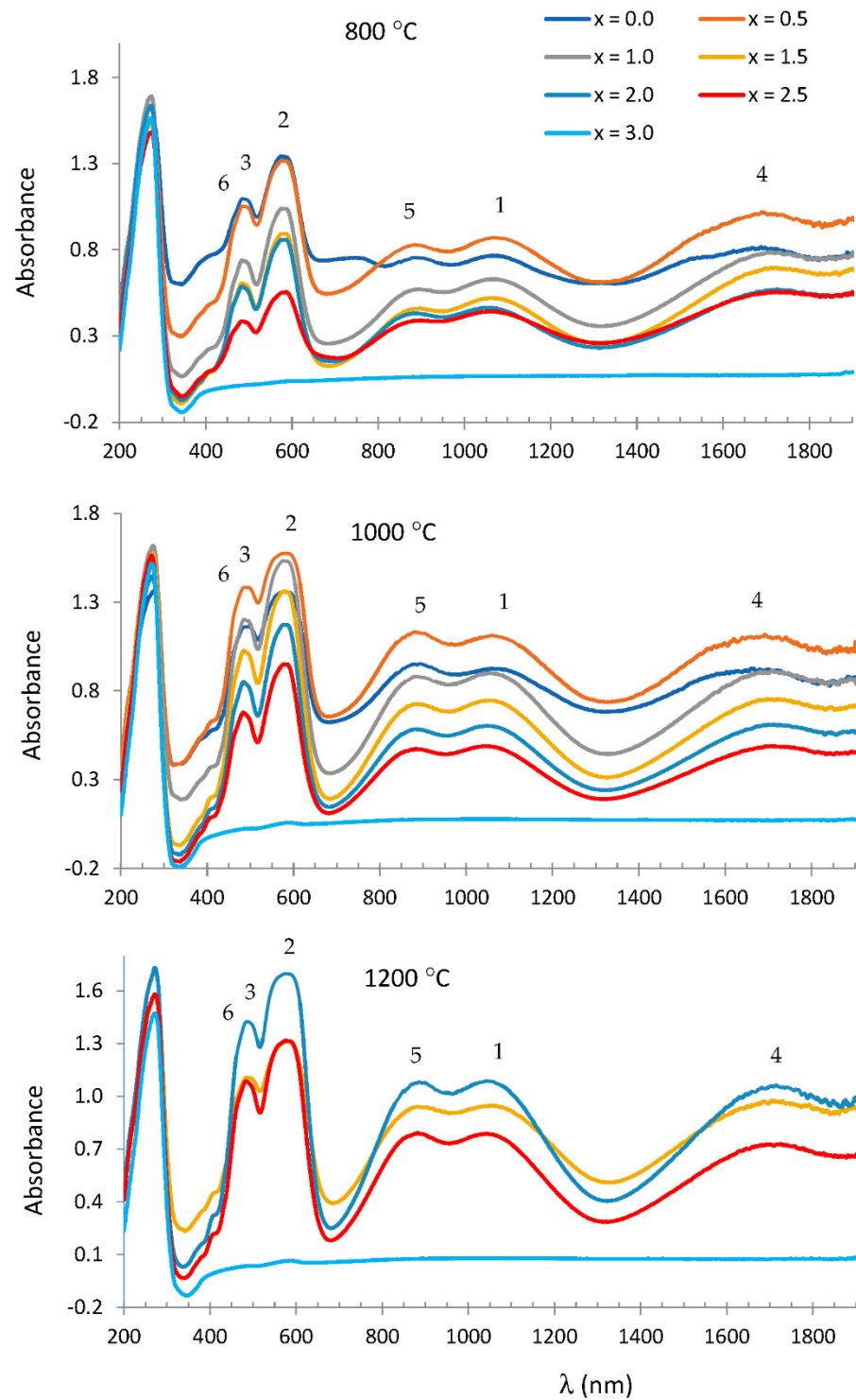
Figure 6. UV–vis–NIR spectra of $Mg_xCo_{3-x}P_2O_8$ fired at 800, 1000 and 1200 °C. Co(II) CN = 6: (1) $^4T_1 \rightarrow ^4T_2$, (2) $^4T_1 \rightarrow ^4A_2$, (3) $^4T_1 \rightarrow ^4T_1(P)$. Co(II) CN = 5:, (4) $^4A_2 \rightarrow ^4A_1$, (5) $^4A_2 \rightarrow ^4E$, (6) $^4A_2 \rightarrow ^4E(P)$.

Table 5. CIE L*a*b* parameters of the $Mg_xCo_{3-x}P_2O_8$ compositions.

x.		Raw Material	300 °C	600 °C	800 °C	1000 °C	1200 °C
0.0	L*	51.36	32.62	35.23	36.73	31.07	
	a*	7.72	8.62	7.64	9.52	16.22	
	b*	−24.72	−11.72	−10.64	−11.50	−20.05	
	Colour	Violet	Purple	Dark violet	Dark violet	Purple	
0.5	L*	49.71	31.21	34.54	37.07	29.30	
	a*	6.00	7.88	10.72	14.57	15.72	
	b*	−30.36	−18.94	−22.32	−20.45	−16.98	
	Colour	Violet	Purple	Purple	Purple	Purple	
1.0	L*	37.31	44.69	51.37	52.43	35.18	
	a*	7.78	4.06	12.73	16.58	24.48	
	b*	−29.41	−27.07	−25.60	−23.25	−23.78	
	Colour	Violet	Violet	Violet	Violet	Purple	
1.5	L*	47.92	48.86	60.12	58.20	41.39	36.24
	a*	5.35	−2.54	15.05	17.52	26.21	18.62
	b*	−20.70	−38.37	−23.98	−24.11	−25.70	−18.33
	Colour	Violet	Blue	Violet	Violet	Violet	Purple
2.0	L*	40.20	60.85	59.14	58.97	49.49	31.33
	a*	−1.83	−10.40	14.03	16.26	24.25	30.93
	b*	−41.74	−30.24	−23.17	−22.42	−24.39	−22.79
	Colour	Blue	Blue	Violet	Violet	Violet	Purple
2.5	L*	54.41	64.37	68.93	68.73	56.60	38.86
	a*	−2.81	−24.25	3.77	7.54	20.30	31.58
	b*	−36.03	−29.37	−14.87	−15.13	−21.20	−24.17
	Colour	Blue	Light blue	Lilac	Lilac	Violet	Purple
3.0	L*	93.89	93.31	95.35	95.38	94.90	94.24
	a*	−0.10	−0.04	−0.15	−0.10	0.29	0.35
	b*	+0.38	+1.12	0.16	0.05	−0.48	−0.54
	Colour	White	White	White	White	White	White
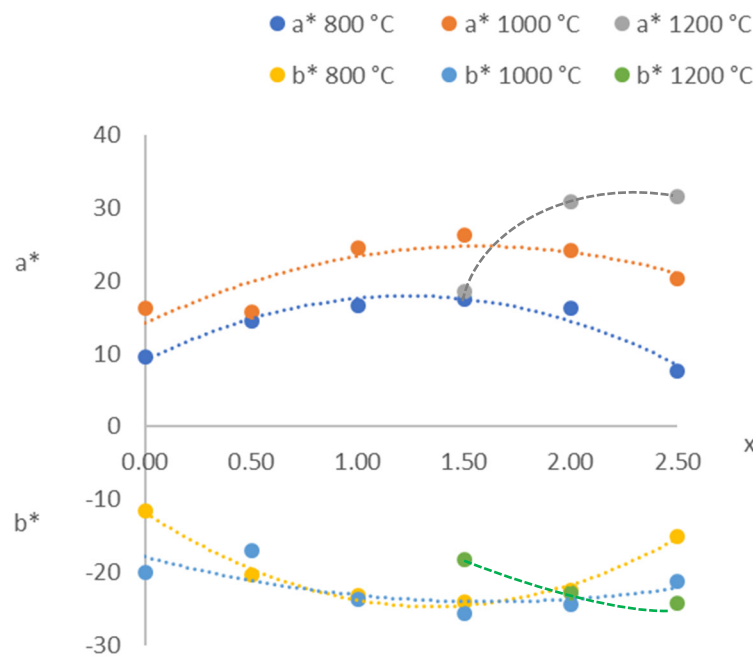


Figure 7. CIE L* a* b* from the $Mg_xCo_{3-x}P_2O_8$ compositions fired at 800, 1000 and 1200 °C.

The colour parameters of the powdered $Mg_xCo_{3-x}P_2O_8$ (1.5 ≤ x ≤ 2.5) solid solutions in this study—with a* of 18.62 to 31.58 and b* of −18.33 to −24.17 (Table 5)—were, in

absolute value, greater than those of the $Co_xZn_{2-x}SiO_4$ compositions ($1.5 \leq x \leq 2.0$ with the olivine structure and $0.05 \leq x \leq 1.00$ with the willemite structure), which had a* of -9.3 to 4.4 and b* of -1.8 to -20.3 [15], and all of them were fired at 1200 °C. A greater amount of red colour (+a*) that was comparable with the greater amount of blue colour (-b*) was obtained in the solid solutions with the stable $Co_3P_2O_8$ structure. So, the powdered $Mg_{2.5}Co_{0.5}P_2O_8$ composition fired at 1200 °C considerably reduced the amount of cobalt, keeping a colour comparable with that in the $Co_3P_2O_8$ pigment, and its melting point was higher than 1200 °C. This composition could be used as a violet inorganic pigment in substitution for the $Co_3P_2O_8$ inorganic pigment, thus decreasing its toxicity due to large amount of cobalt. $Co_3P_2O_8$ is classified as a pigment (DCMA-8-11-1, DCMA Classification of Mixed Metal Oxide Inorganic Colour Pigments). Pigments include naturally occurring substances prepared from minerals or their combustion products, as well as synthetic compounds produced from appropriate raw materials. Pigments are insoluble in the surrounding media, and their optical effect arises from selective light absorption [19]. Therefore, the solid solutions prepared here are also inorganic pigments when unglazed.

Figure 8 shows the visible spectra in glazed tiles prepared with 3% $Mg_xCo_{3-x}P_2O_8$ ($1.5 \leq x \leq 3.0$) materials fired at 1200 °C. The bands assigned to Co(II) in the octahedral site and to Co(II) in a square-planar pyramid coordination were detected at higher wavelengths in the enamelled samples than in the powdered samples. This displacement increased the absorbance in the range of 593–650 nm and slightly decreased the absorbance at about 550 nm, so the colour observed in these enamelled materials was the characteristic cobalt blue colour obtained from purple powdered materials ($1.5 \leq x \leq 2.5$). The absorbance between 450 and 630 nm decreased in the enamelled $Co_3P_2O_8$ composition with respect to the powdered $Co_3P_2O_8$ at 1000 °C. This decrease was not detected in the $Mg_{2.0}Co_{1.0}P_2O_8$ and $Mg_{2.5}Co_{0.5}P_2O_8$ compositions that were fired at 1200 °C with their lower amount of cobalt. The violet colour of the powdered samples changed to the characteristic cobalt blue due to the change in the local environment of the Co(II) ions, which could be visualised in the UVV spectra of the glazed samples with the displacement of the bands towards higher wavelengths and with the appearance of a new band assigned to tetrahedral Co(II). This blue colour was also obtained with Co_2SiO_4, $MgCoSiO_4$ or $Co_3P_2O_8$ pigments containing a greater amount of cobalt.
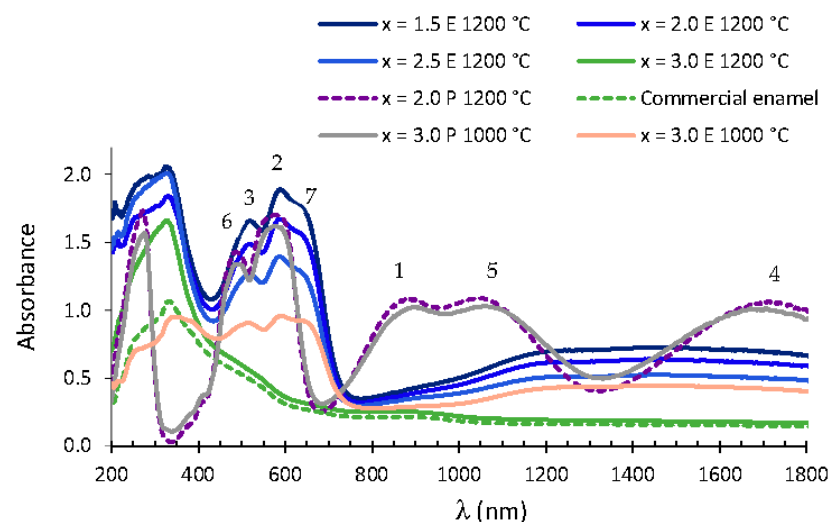
Figure 8. UV–vis–NIR spectra of 3% $Mg_xCo_{3-x}P_2O_8$ ($0.0 \leq x \leq 3.0$) compositions fired at 1200 °C and the commercial enamel and composition fired at 1000 °C with x = 3.0. E: enamelled sample. P = powdered sample. Co(II) CN= 6: (1) $^4T_1 \rightarrow {}^4T_2$, (2) $^4T_1 \rightarrow {}^4A_2$, (3) $^4T_1 \rightarrow {}^4T_1(P)$. Co(II) CN = 5: (4) $^4A_2 \rightarrow {}^4A_1$, (5) $^4A_2 \rightarrow {}^4E$, (6) $^4A_2 \rightarrow {}^4E(P)$. Co(II) CN = 4 (tetrahedral coordination): (7) $^4A_2 \rightarrow {}^4T_1(P)$.

The colour parameters (L* a* b*) of the enamelled samples under the conditions of this study with the commercial glaze used are included in Table 6. A dark blue colour was obtained from the compositions with $1.5 \leq x \leq 2.0$, and a blue colour with a greater lightness was obtained from the composition with $x = 2.5$. The $Mg_xCo_{3-x}P_2O_8$ ($1.5 \leq x \leq 2.5$) solid solutions with the stable $Co_3P_2O_8$ structure may be used as blue pigments in the ceramic industry. The CIE L*/a*/b* colour parameters of classical blue pigments used in the ceramic industry with Co_2SiO_4 or $MgCoSiO_4$ compositions with an olivine structure (weight ratio of pigment to glaze equal to 1:5, 20 weight% pigment) were 29.00/11.20/–25.6 and 29.19/7.97/–17.61, respectively, for the single-fired enamelled samples [20,21]. The glazed tiles from the $Mg_xCo_{3-x}P_2O_8$ ($1.5 \leq x \leq 2.5$) solid solutions (including 3% pigment) showed blue colourations with a large amount of blue colour ($-15.9 \leq b^* \leq -20.20$) and a low lightness ($18.53 \leq L^* \leq 27.05$). The amount of cobalt in the compositions was between 28.1 weight% ($x = 1.5$) and 10.5 weight% ($x = 2.5$), while it was 56.1 weight% in Co_2SiO_4 and 33.6 weight% in $MgCoSiO_4$. The use of the $Mg_xCo_{3-x}P_2O_8$ ($1.5 \leq x \leq 2.5$) solid solutions with the stable $Co_3P_2O_8$ structure as blue pigments reduced the amount of cobalt used with respect to the amount of cobalt used in Co_2SiO_4 and $MgCoSiO_4$ pigments because comparable values of blue (negative b*) were obtained with a smaller amount of cobalt in the composition of the pigment and with a pigment quantity that was lower by 6.7.

Table 6. CIE L* a* b* colour parameters from the glazed tiles obtained from the $Mg_xCo_{3-x}P_2O_8$ ($1.5 \leq x \leq 3.0$) materials fired at 1200 °C.

x	L*	a*	b*	Observed Colour
1.5	18.53	−0.24	−26.18	Dark blue
2.0	20.56	+0.00	−20.20	Dark blue
2.5	27.05	+0.55	−15.95	Blue
3.0	68.24	+13.22	+26.94	Beige

4. Conclusions

$Mg_xCo_{3-x}P_2O_8$ ($0 \leq x \leq 3$) solid solutions with the stable $Co_3P_2O_8$ structure were synthesised via the chemical coprecipitation method. Their structural characterisation is consistent with the replacement of the Co(II) ion with the smaller Mg(II) ion. A decrease in the b unit cell parameter and the unit cell volume with x was obtained. The slight increase in the a and c unit cell parameters with x indicates that the $Co_3P_2O_8$ structure is distorted when Mg(II) is incorporated into it. When $x > 1.0$, the decrease in the longest M-O distance with x is remarkable.

The experimental distribution of Co(II) between the two positions in the solid solutions with the stable $Co_3P_2O_8$ structure indicates that the Co(II) ion presents a preference for the site with CN = 5 (4e) and the Mg(II) ion presents a preference for the octahedral position (2a). The bands in the UV–vis–NIR spectra can be assigned to Co(II) in octahedral and square-planar pyramid coordination. The most noticeable decrease in absorbance with composition in the spectra was due to the decrease in the total Co(II) in the compositions. A slight decrease in the absorbance from the first transition, which was assigned to Co(II) in the octahedral site, with respect to the transition assigned to Co(II) in a square-planar pyramid coordination was also detected.

Purple and violet colours were obtained when a stable $Co_3P_2O_8$ structure was developed from $Mg_xCo_{3-x}P_2O_8$ ($0 \leq x \leq 3$) compositions. These colourations were kept at 1000 and 1200 °C when $x \geq 1.5$, so inorganic pigments with a smaller amount of Co(II) were obtained. From powdered samples, optimal compositions can be established when $2.0 \leq x \leq 2.5$ (highest a* and lowest b*) at this temperature. This highlights the purple colour with the values of a* = 31.6 and b* = –24.2 obtained from the powdered $Mg_{2.5}Co_{0.5}P_2O_8$ composition fired at 1200 °C, which minimised the amount of cobalt and improved both the thermal stability and the colour of the $Co_3P_2O_8$ pigment. $Mg_xCo_{3-x}P_2O_8$ ($2.0 \leq x \leq 2.5$) solid solutions are considered the optimal compositions for obtaining the characteristic cobalt blue in glazed tiles.

References

1. *Inorganic Crystal Structure Database (ICSD Web)*; Fachinformationszentrum (FIZ): Karlsruhe, Germany, 2021.
2. DCMA. *Classification and Chemical Description of the Mixed Metal Oxide Inorganic Coloured Pigments*, 2nd ed.; Metal Oxides and Ceramics Colors Subcommittee, Dry Color Manufacturer's Ass.: Washington, DC, USA, 1982.
3. Sarver, J.F. Figure. 2309. System CoO-Co(PO$_3$)$_2$. *Trans. Brit. Ceram. Soc.* **1966**, *65*, 196.
4. Tena, M.A.; Mendoza, R.; Trobajo, C.; García, J.R.; García-Granda, S. Ceramic pigments from Co$_x$Ni$_{3-x}$P$_2$O$_8$ ($0 \leq x \leq 3$) solid solutions. *Ceram. Int.* **2021**, *47*, 29888–29899. [CrossRef]
5. Roczniki, J.B. Figure 272. System MgO-P$_2$O$_5$. *Chemistry* **1958**, *32*, 19.
6. Thejus, P.K.; Koley, B.; Nishanth, K.G. An intense purple chromophore based on Co2+ in distorted tetrahedral coordination. *Dyes Pigm.* **2018**, *158*, 267–276. [CrossRef]
7. Nord, A.G.; Stefanidis, T. Structure Refinements of Co3(PO4)2. A Note on the Reliability of Powder Diffraction Studies. *Acta Chem. Scand.* **1983**, *A37*, 715–721. [CrossRef]
8. Junghwa, H.; Seungwan, S.; Seungtae, H. Strontium magnesium phosphate, Sr$_2$ + xMg$_3$-xP 4O15 (x ~ 0.36), from laboratory X-ray powder data. *Acta Cryst.* **2011**, *C67*, i1–i3. [CrossRef]
9. Rietveld, H.M. A profile refinement method for nuclear and magnetic structures. *J. Appl. Crystallogr.* **1969**, *2*, 65–71. [CrossRef]
10. Rodriguez-Carvajal, J. (September 2018-ILL-JRC). *Fullprof.2k Computer Program*, version 6.50 France; 2018. Available online: http://www.ill.eu/sites/fullprof/ (accessed on 16 January 2022).
11. Chapon, L.; Rodriguez-Carvajal, J. *FPStudio Computer Program, version 2.0*; Rutherford Appleton Laboratory: Oxfordshire, UK; Institut Laue Langevin: Grenoble, France, 2008.
12. Nord, A.G.; Stefanidis, T. The cation distribution in two (Co, Mg)$_3$(PO$_4$)$_2$ solid solutions. *Z. Fur Krist.* **1980**, *153*, 141–149. [CrossRef]
13. Nord, A.G.; Stefanidis, T. The cation distribution between five- and six-coordinated sites in some (Mg, Me)$_3$(PO$_4$)$_2$) solid solutions. *Mat. Res. Bull.* **1980**, *15*, 1183–1191. [CrossRef]
14. Aaddane, A.; Kacimi, M.; Ziyad, M. Oxidative dehydrogenation of ethane and propane over magnesium–cobalt phosphates CoxMg3−x(PO4)2. *Catal. Lett.* **2001**, *73*, 47–53. [CrossRef]
15. Forés, A.; Llusar, M.; Badenes, J.A.; Calbo, J.; Tena, M.A.; Monrós, G. Cobalt minimisation in willemite (Co$_x$Zn$_{2−x}$SiO$_4$) ceramic pigments. *Green Chem.* **2000**, *2*, 93–100. [CrossRef]
16. Commission Internationale del'Eclairage. Recommendations on Uniform Color Spaces, Color Difference Equations, Phychometrics Color Terms. 1978. In *Supplement No. 2 of CIE Publication No. 15 (E1-1.31)*; Bureau Central de la CIE: Paris, France, 1971.
17. West, A.R. *Solid State Chemistry and Its Applications*; John Wiley & Sons: Chichester, UK, 1984.
18. Lever, A.B.P. *Inorganic Electronic Spectroscopy*, 2nd ed.; Elsevier Science B. V.: Amsterdam, The Netherlands, 1977; pp. 507–511.
19. Jesionowski, T.; Ciesielczyk, F. Inorganic, Hybrid and Functional Pigments. In *Encyclopedia of Color Science and Technology*; Shamey, R., Ed.; Springer: Berlin/Heidelberg, Germany, 2021. [CrossRef]
20. Llusar, M.; Forés, A.; Badenes, J.A.; Tena, M.A.; Monrós, G. Colour analysis of some cobalt-based blue pigments. *J. Eur. Ceram. Soc.* **2001**, *21*, 1121–1130. [CrossRef]
21. Molinari, C.; Conte, S.; Zanelli, C.; Ardit, M.; Cruciani, G.; Dondi, M. Ceramic pigments and dyes beyond the inkjet revolution: From technological requeriments to constraints in colorant design. *Ceram. Int.* **2020**, *46*, 21839–21872. [CrossRef]